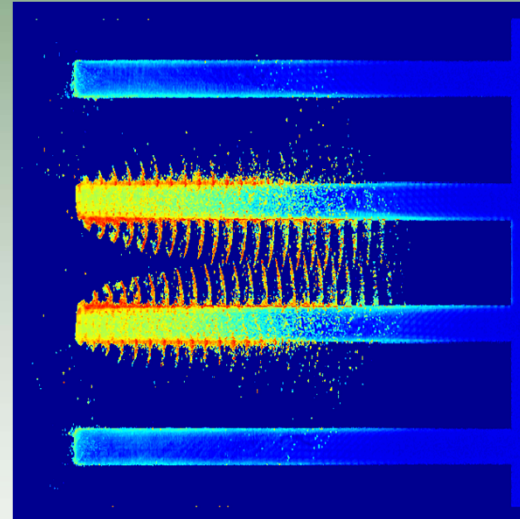
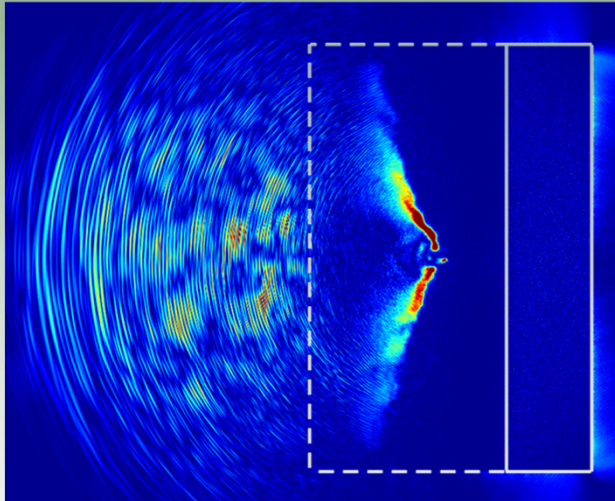


# *Using the particle-in-cell (PIC) method to model the strong field laser-plasma interaction*



**Douglass Schumacher**  
**Department of Physics**  
**The Ohio State University**



**ELI-NP School**  
**September 21-25, 2015**  
**Bucharest, Romania**

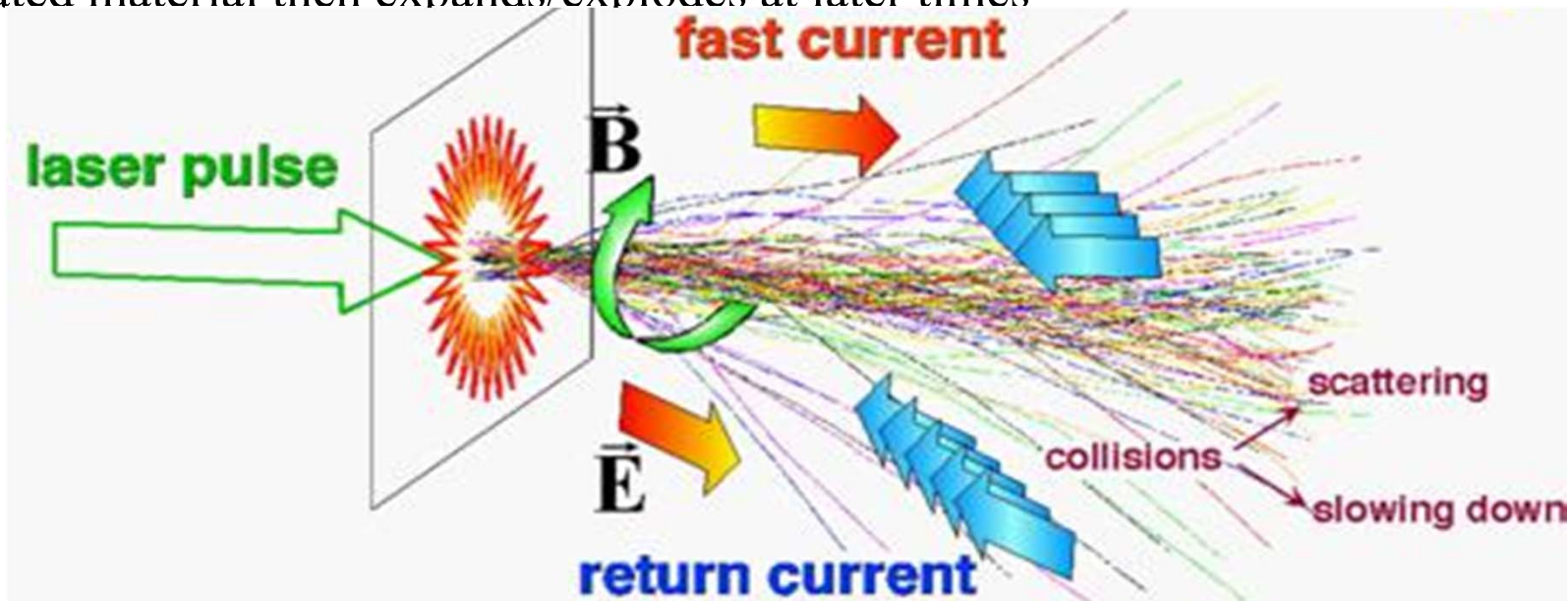
# Outline



- 1. Goals, Scope and Motivation**
2. Particle-in-cell Method
3. Case Studies

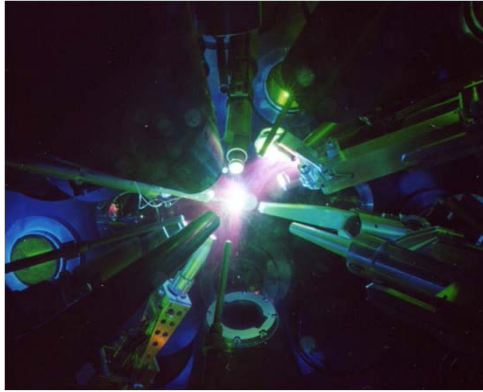
# The laser plasma interaction (LPI) problem

- Consider intense short laser pulse: relativistic,  $a > 1$  or  $I \gtrsim 10^{18} \text{ W/cm}^2$  for  $1 \mu\text{m}$  light
- Initial coupling to relativistic electrons (hot electrons)
- Energetic electrons
  - Carry energy into/through material
  - Lose energy to ions
  - Lose energy to radiation
  - Drives cold return current
- Heated material then expands/explodes at later times



PIC Simulation; Gremillet, et. al, POP 9, 941 (2002)

# The role of numerical simulations



<http://hedp.physics.ucla.edu/images/omega.jpg>

$$\begin{aligned}\vec{\nabla} \times \vec{E} &= -\frac{\partial \vec{B}}{\partial t} \\ \vec{\nabla} \times \vec{B} &= \mu_0 \vec{J} + \mu_0 \epsilon_0 \frac{\partial \vec{E}}{\partial t} \\ \vec{\nabla} \cdot \vec{E} &= \frac{\rho}{\epsilon_0} \\ \vec{\nabla} \cdot \vec{B} &= 0 \\ \frac{\partial \vec{p}}{\partial t} &= q(\vec{E} + \vec{v} \times \vec{B})\end{aligned}$$



## Experiment: The final arbiter, but...

- How are experiments designed?
- Diagnostics tend to be indirect measures (eg.  $K_\alpha$  or CTR for the hot electron distribution)
- Diagnostics tend to be time-integrated
- Exp. apparatus can be difficult to characterize

## Theory: Have fundamental motion eqns. but...

- We can't solve them in full
- Less trivially, its difficult to identify useful regimes where approximations are accurate
- Some of our most interesting questions lie in very messy regimes (eg. xray opacity in stellar interiors)

## Simulations: Complementary

- Model (proposed) experiments including synthetic diags.
- Can examine predictions of theory under ideal conditions as simplified test (compared to experiment)
- Can explore situations for which there is no good theory

## Goals

- Provide introduction to PIC
- Learn what it can do and the compromises that are often made
- Become critical readers of the literature
- Facilitate your entry to PIC modeling, should you need or wish to try it

Two classic texts that are good for getting started and for reference:

- C. K. Birdsall and A. B. Langdon, **Plasma Physics Via Computer Simulation**, Taylor & Francis, New York (2005);  
ISBN-13: 978-0750310253
- R. W. Hockney and J. W. Eastwood, **Computer Simulation Using Particles**, McGraw-Hill, New York (1981);  
ISBN-13: 978-0070291089

A number of PIC codes are now available for use at no cost. Here is a popular one:

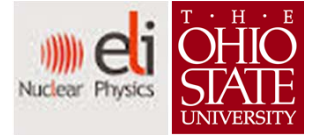
- EPOCH      <https://ccpforge.cse.rl.ac.uk/gf/project/epoch/>  
(registration required, switching to a new site)

# Outline



1. Goals, Scope and Motivation
2. **Particle-in-cell Method**
  - a) **Fundamentals – the basic method**
  - b) Constraints
  - c) Other aspects of a working simulation
  - d) Issues for the Laser Plasma Interaction
3. Case Studies

# Equations of motion: Maxwell eqns. and Lorentz force law



$$\vec{\nabla} \times \vec{E} = -\frac{\partial \vec{B}}{\partial t}$$

$$\vec{\nabla} \cdot \vec{E} = \frac{\rho}{\epsilon_0}$$

$$\vec{\nabla} \times \vec{B} = \mu_0 \vec{J} + \mu_0 \epsilon_0 \frac{\partial \vec{E}}{\partial t}$$

$$\vec{\nabla} \cdot \vec{B} = 0$$

- Fields evaluated over all space and time
- Time evolution is due to currents and changing fields

$$\frac{d\vec{p}}{dt} = q(\vec{E} + \vec{v} \times \vec{B})$$

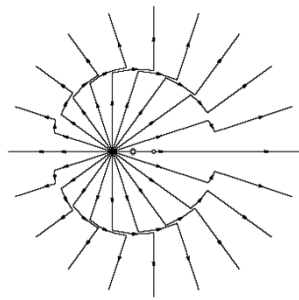
- Evaluated for all particles
- General for non-quantum mechanical systems; fully relativistic.
- Ionization, recombination, scattering, material resistivity, opacity and similar are often important and then must be introduced, but we neglect for now.
- Electrostatic case (so non-relativistic):

$$\text{only } \vec{\nabla} \cdot \vec{E} = \frac{\rho}{\epsilon_0} \text{ or } \nabla^2 \phi = \frac{\rho}{\epsilon_0} \text{ and } \frac{\partial \vec{p}}{\partial t} = q\vec{E} \text{ required}$$

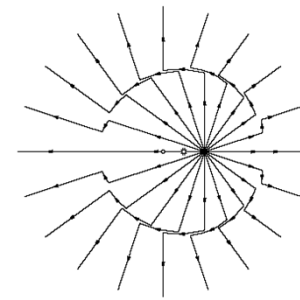
Consider electrostatic case and a fully ionized copper plasma with  $10 \mu\text{m} \times 10 \mu\text{m} \times 100 \mu\text{m}$ .  
 $m \approx 0.90 \text{ g}$  or  $N_{\text{mol}} \approx 14 \text{ nmol}$  so  $N_{\text{ion}} \approx 9 \times 10^{15}$  ions and  $N_e = Z N_{\text{ion}}$  with  $Z = 28$ .  
Number of force pair calculations for electrons alone is roughly  $N_e^2 \approx 10^{34}$ .  
At 1 calc/cycle and 1000 3 GHz processors, that would take roughly  $10^{15}$  years.



# Discretization of the fields (PIC)

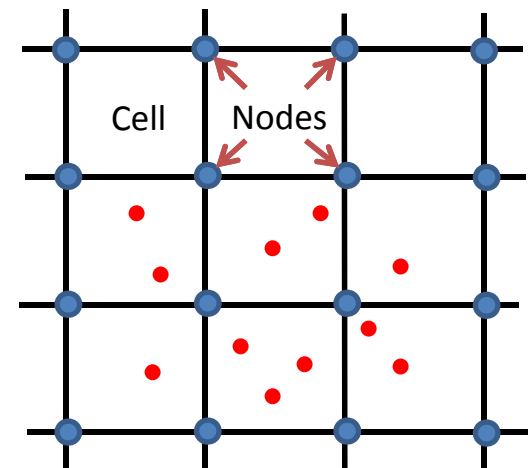


charges  $\longleftrightarrow$  fields  $\longleftrightarrow$  charges

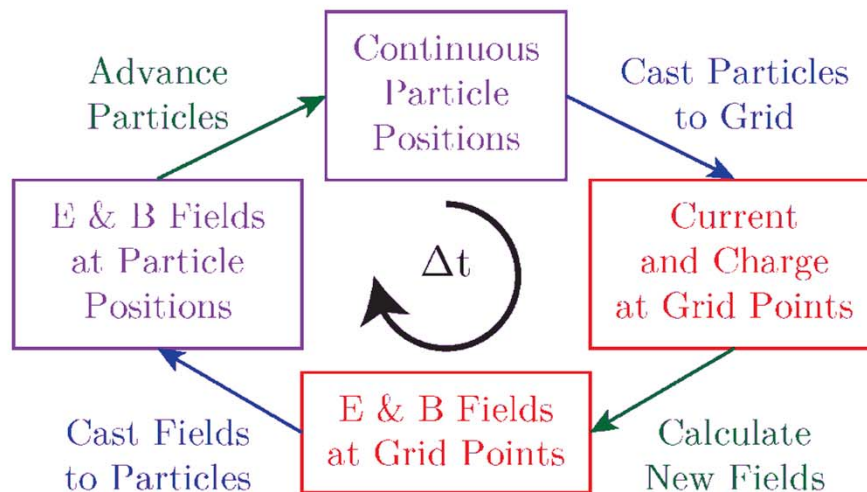


PIC discretizes field evolution at the nodes of cells leaving particle position continuous.

The equations of motion are local so, to update the fields, we need the currents carried by the particles represented at the nodes and vice versa.



This suggests the following PIC cycle:



For  $N$  particles and  $M$  grid points  
 Cast to the grid  $\sim N/M * M = N$   
 Advance fields  $\sim M$   
 Interpolate and push particles  $\sim N$



# Macroparticles (PIC)

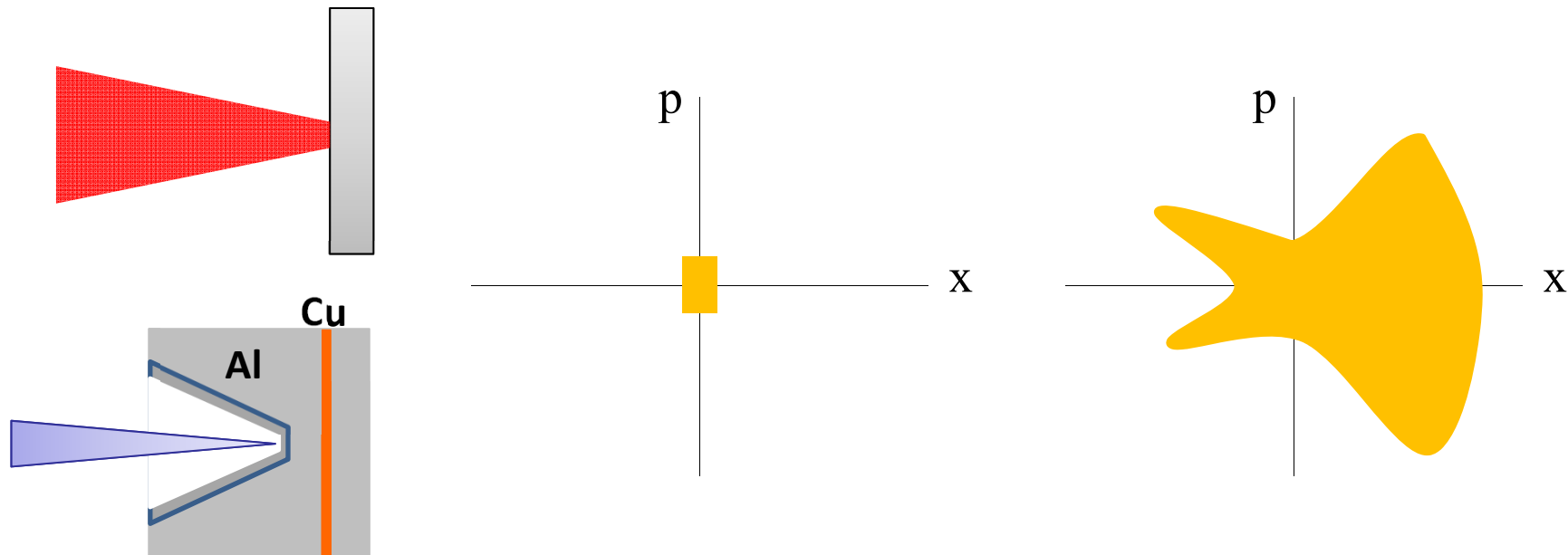
We represent the true population of a species  $s$  (electrons,  $\text{Cu}^+$ , ...) using macroparticles:  
 $q = w q_s$  and  $m = w m_s$  where  $w$  is the “particle weight”, a positive integer.

$$q/m = q_s/m_s \quad \text{and} \quad \frac{d\gamma\vec{v}}{dt} = \frac{q}{m} (\vec{E} + \vec{v} \times \vec{B}) \quad \text{so, the eqns. of motion are preserved.}$$

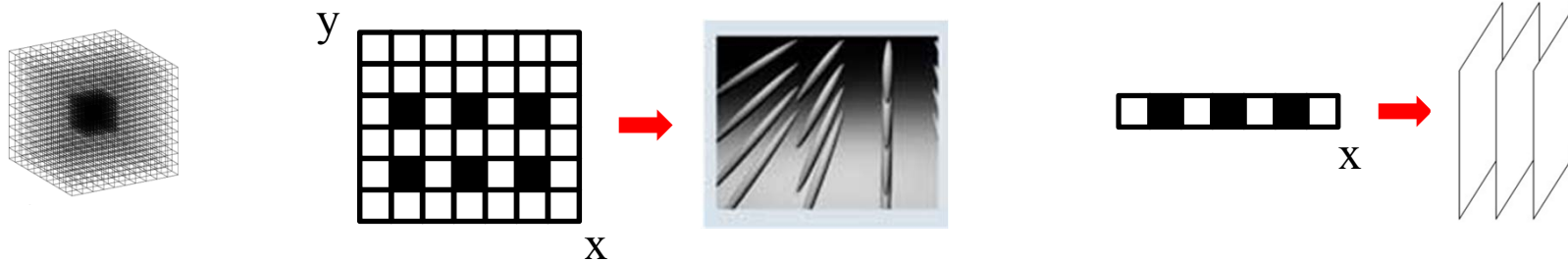
$w$  is often large,  $10^{10}$  or higher, and the number of macroparticles used does not generally exceed several billion. In fact, it is frequently much less.

The use of macroparticles is effectively a sampling of phase space.

The initial macroparticle weight can even vary with position or change dynamically.

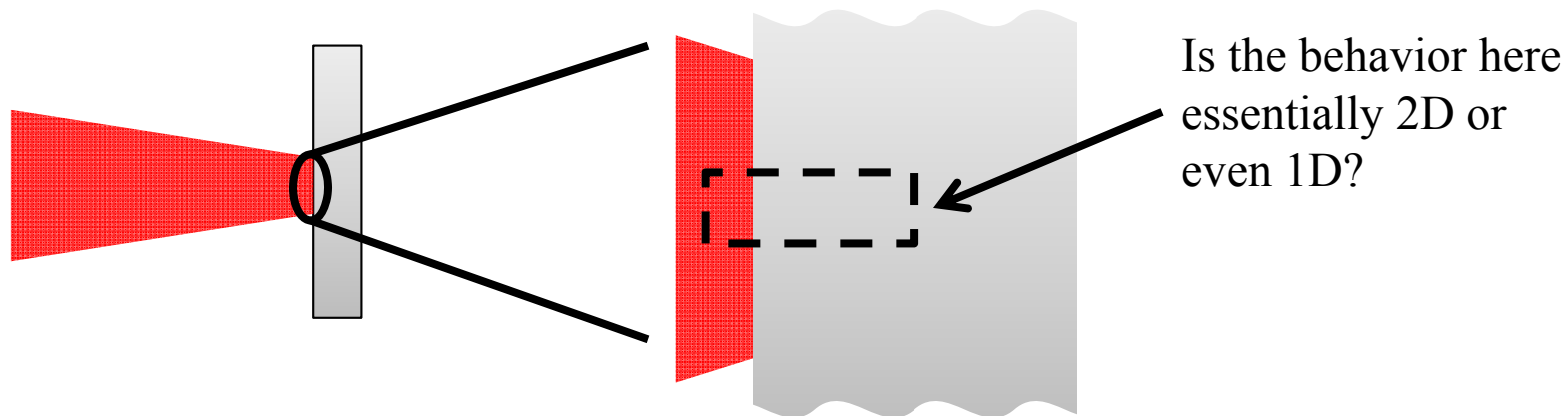


# Dimensionality



We often restrict dimensionality out of computational necessity.

This might be justified depending on the problem symmetry or, more simply, we might be willing to accept the loss in realism in order to get a result.

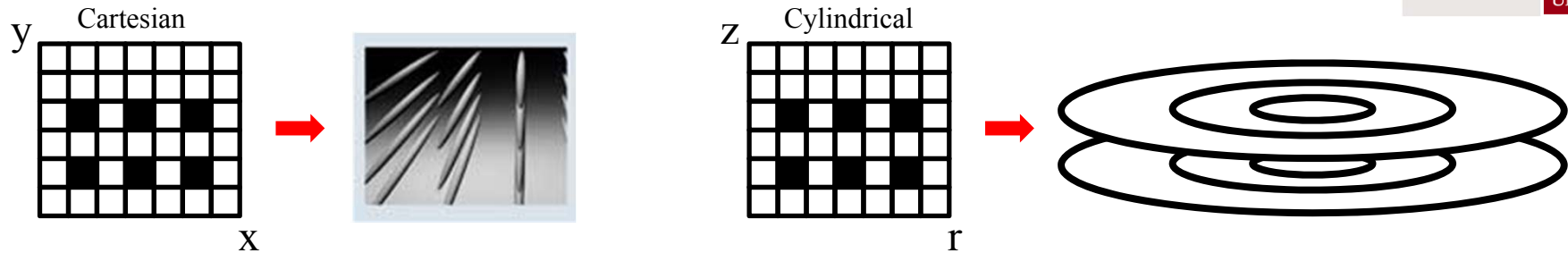


Example from electrostatics: a “point” charge in 2D:

$$\nabla^2 \phi = \frac{\rho}{\epsilon_0} = \epsilon_0 \lambda \delta(\vec{x}) = \epsilon_0 \lambda \delta(x) \delta(y) \Rightarrow \phi = -\frac{\lambda}{2\pi\epsilon_0} \ln|\vec{x}|$$

$$E = \frac{\lambda}{2\pi\epsilon_0} \frac{1}{|\vec{x}|}$$

# More on working in restricted dimensions



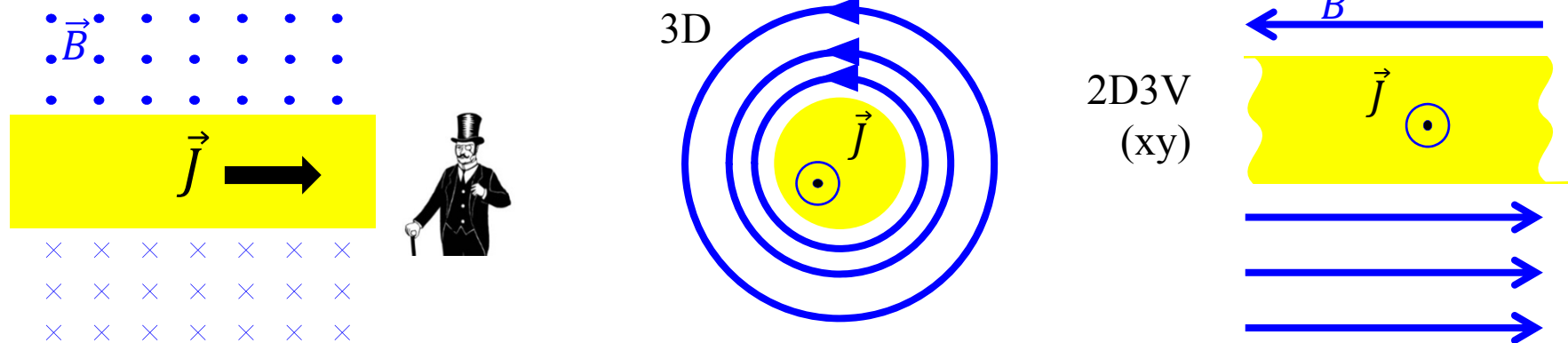
And similarly for other possibilities ( $r, \theta$ ) or coordinate systems (spherical).  
 Not all possibilities are implemented by all (or even any) PIC codes, but some are.  
 For close range interactions, this may not matter, but at long range it will.

## 1D3V, 2D3V or 2½D

Working in restricted dimension means we will not evaluate the appropriate spatial derivatives.

Vectors can retain all degrees of freedom, however:  $\vec{p}, \vec{J}, \vec{E}, \vec{B}$

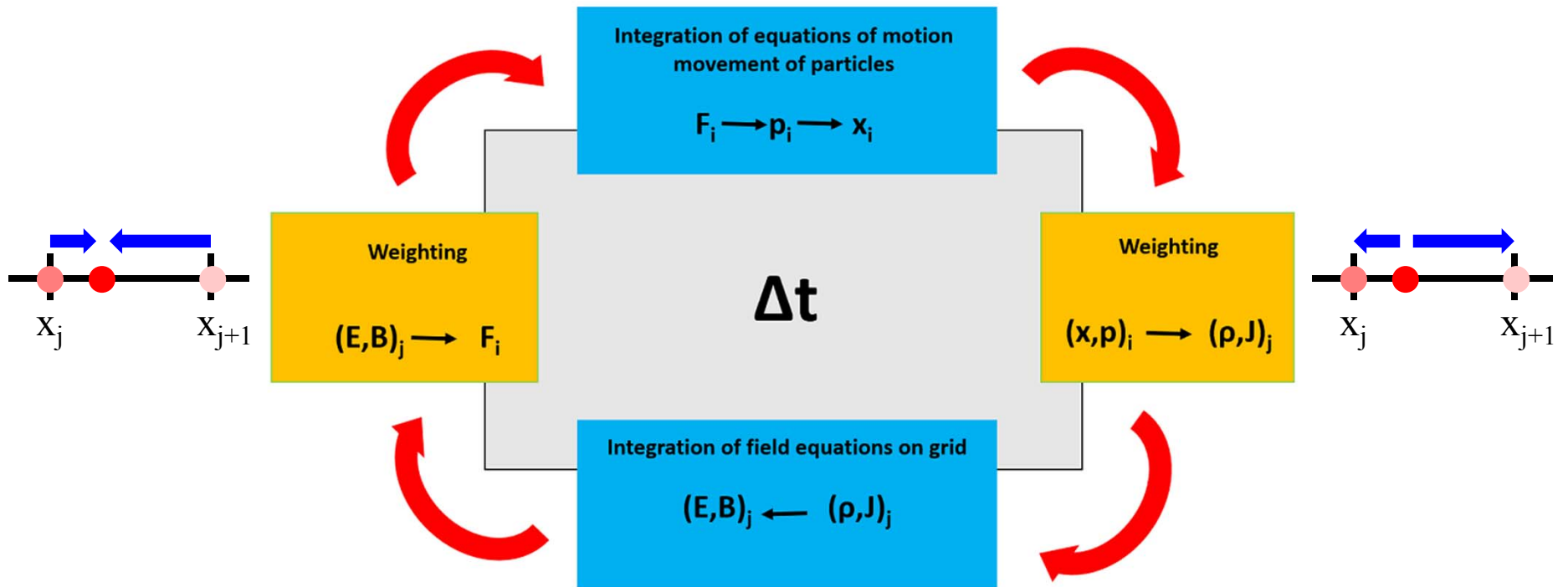
Again, note geometric effects of field variation with distance :



This means we can still have self-consistent, self-propagating EM waves in 1D3V and 2D3V, but not in all coordinate systems (eg. Cartesian  $(x, xy)$  not cylindrical  $(z, rz)$ ).

# PIC Cycle (time step) → Implementation

$$\frac{d\vec{p}}{dt} = q(\vec{E} + \vec{v} \times \vec{B})$$



$$\vec{\nabla} \times \vec{E} = -\frac{\partial \vec{B}}{\partial t}$$

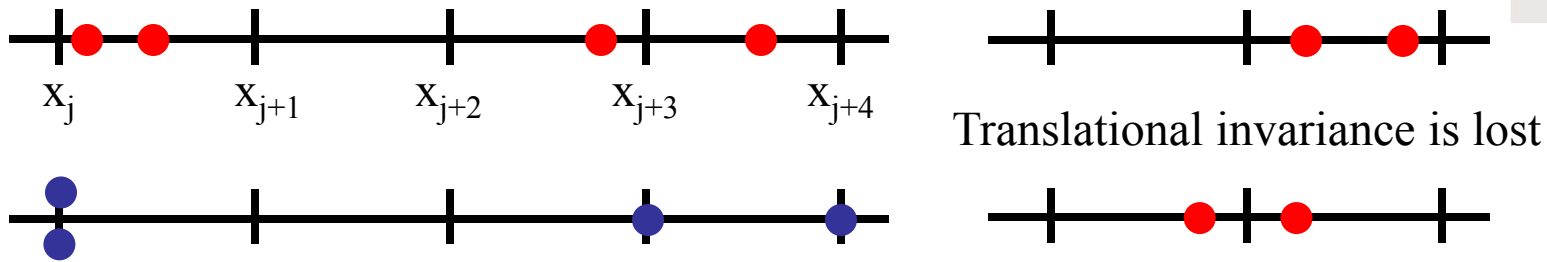
$$\vec{\nabla} \times \vec{B} = \mu_0 \vec{J} + \mu_0 \epsilon_0 \frac{\partial \vec{E}}{\partial t}$$

Notation (this figure only)

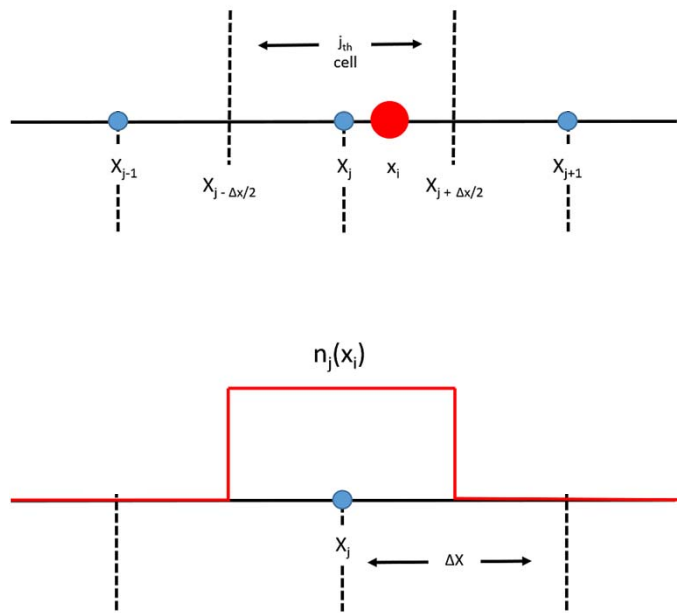
$i \rightarrow$  particle

$j \rightarrow$  node

# Weighting – Nearest Grid Point (0<sup>th</sup> order)

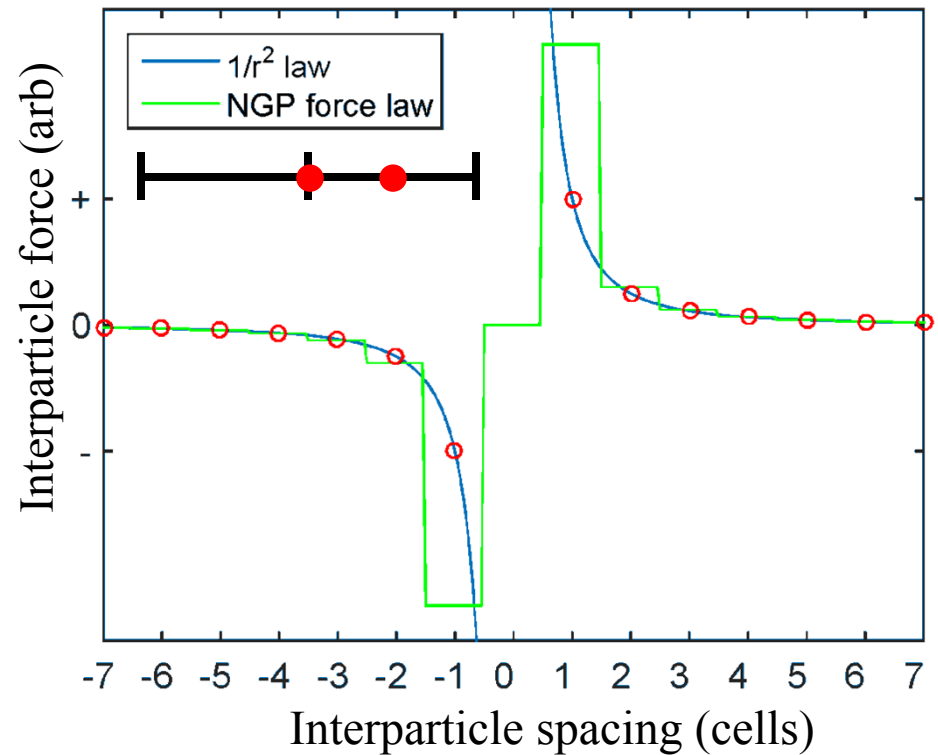


Shape function  $S$



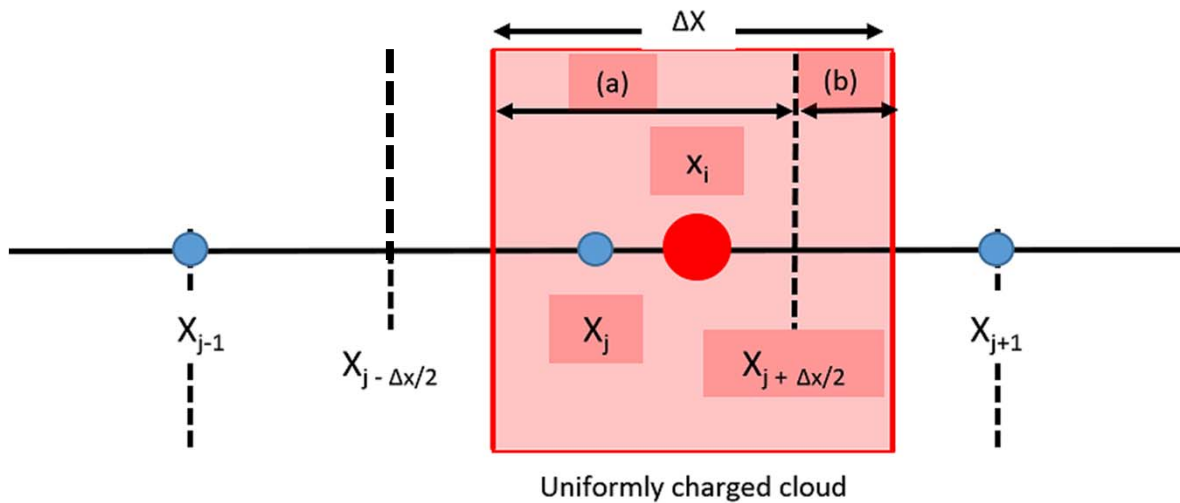
Noisy...

Electrostatic force with one particle at a node



PIC achieves Debye shielding (long range effect) without using a large number of particles.

# Weighting – Cloud-in-Cell (1<sup>st</sup> order)

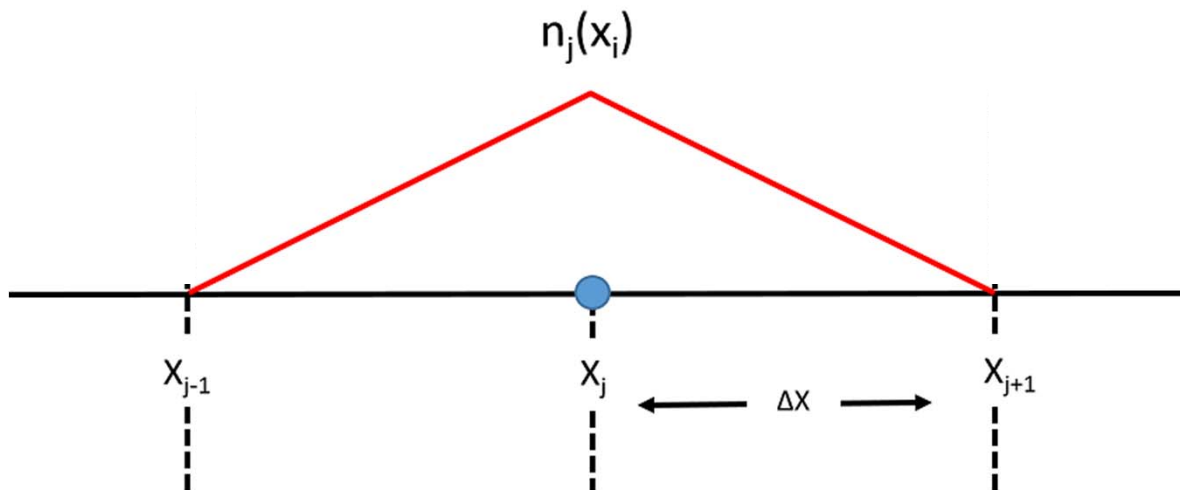


$$q_j = q \frac{X_{j+1} - x_i}{\Delta X}$$

$$q_{j+1} = q \frac{x_i - X_j}{\Delta X}$$

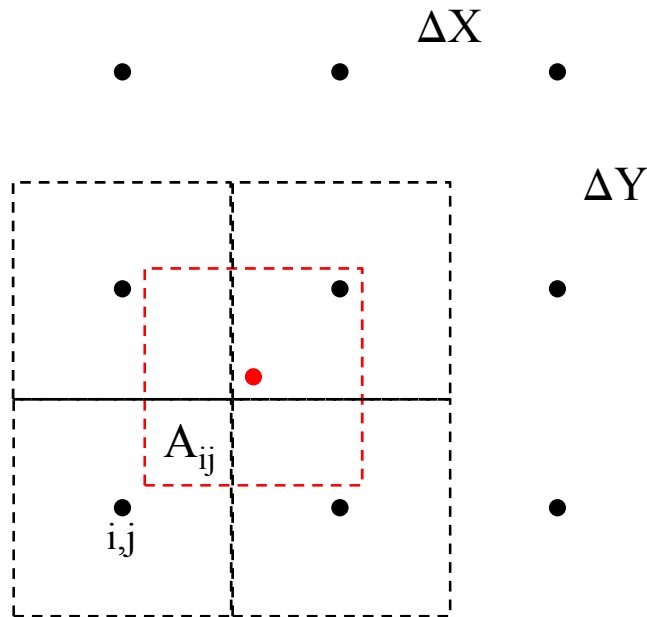
To eliminate self-forces, you interpolate the fields using the same weighting as the particles

$$E_i = \frac{X_{j+1} - x_i}{\Delta X} E_j + \frac{x_i - X_j}{\Delta X} E_{j+1}$$



Higher order schemes are used. More on the effect of this later.

# Generalization to 2D using areas (or 3D using volumes)



$$S(\vec{x}_p - \vec{X}_{ij}) = \frac{A_{ij}}{\Delta X \Delta Y}$$

$$\sum_{i,j} S(\vec{x}_p - \vec{X}_{ij}) = 1$$

Let's consider the total system momentum:  $\vec{P}$   
 For simplicity, consider 1D electrostatic problem, so working with charge densities and E-fields:

$$\rho_i = \frac{1}{\Delta x} \sum_p q_p S(\vec{x}_p - \vec{X}_i)$$

$$\vec{E}_p = \sum_i \vec{E}_i S(\vec{x}_p - \vec{X}_i)$$

$$\frac{d\vec{P}}{dt} = \sum_p q_p \vec{E}_p = \sum_p q_p \sum_i \vec{E}_i S(\vec{x}_p - \vec{X}_i)$$

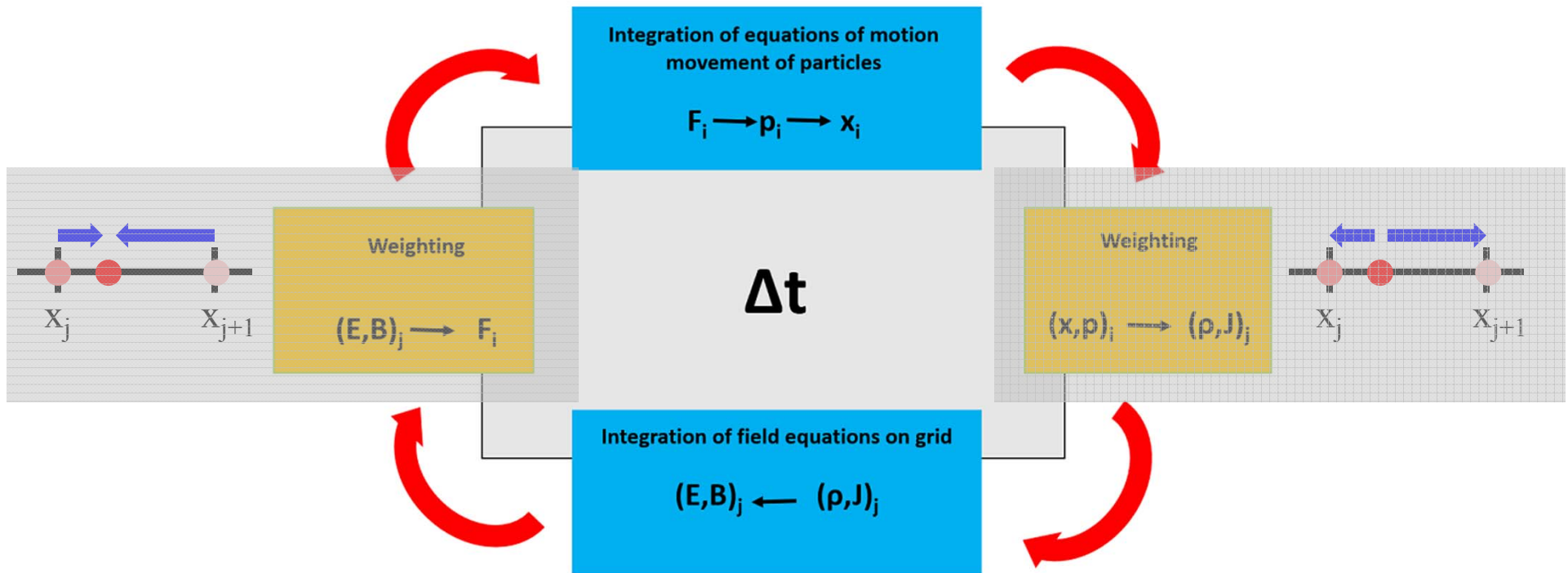
$$\frac{d\vec{P}}{dt} = \Delta x \sum_{i,j} \rho_i \vec{E}_i$$

$$\frac{d\vec{P}}{dt} = 0 \quad \text{For periodic boundary conditions but not for conducting boundaries.}$$



# PIC Cycle (time step) → Implementation

$$\frac{d\vec{p}}{dt} = q(\vec{E} + \vec{v} \times \vec{B})$$



$$\vec{\nabla} \times \vec{E} = -\frac{\partial \vec{B}}{\partial t}$$

$$\vec{\nabla} \times \vec{B} = \mu_0 \vec{J} + \mu_0 \epsilon_0 \frac{\partial \vec{E}}{\partial t}$$

Notation (this figure only)

$i \rightarrow$  particle

$j \rightarrow$  node

# From differential equations of motion to difference equations



Consider a simple example before we turn to our equations of motion:

$$\frac{du}{dt} = -au \quad \text{Let } a > 0 \text{ and } u_0 = u(0) \text{ be the initial condition. } (u(t) = u_0 e^{-at})$$

$$\frac{\Delta u}{\Delta t} \approx -au \quad \text{with time discretized as } t = n\Delta t \text{ so } u(t) = u(n\Delta t) \equiv u_n.$$

There is no unique interpretation of this equation, however. Here are two versions:

## Explicit

$$\frac{u_{n+1} - u_n}{\Delta t} = -au_n$$

$$u_{n+1} = (1 - a\Delta t)u_n$$

With solution at time t:

$$u_n = (1 - a\Delta t)^n u_0$$

This turns out to be inefficient, but it will work unless  $(1 - a\Delta t) < -1$  which diverges.  $u_n$  should always be finite.

We require:  $\Delta t < 2/a$

Note this is a stability issue.

Accuracy is still yet another matter.

## Implicit

$$\frac{u_{n+1} - u_n}{\Delta t} = -au_{n+1}$$

$$u_{n+1} = u_n / (1 + a\Delta t)$$

With solution at time t:

$$u_n = \frac{1}{(1 + a\Delta t)^n} u_0$$

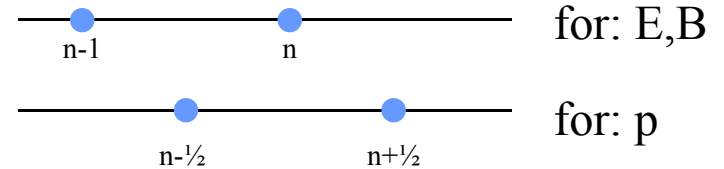
This is unconditionally stable for any value of  $\Delta t$ . We are now free to pick  $\Delta t$  for accuracy. When solving non-trivial equations of motion, implicit solutions tend to be more complicated and require more computation time than explicit solutions.

# Boris Particle Pusher

$$\frac{d\vec{p}}{dt} = q(\vec{E} + \vec{v} \times \vec{B}) \Rightarrow \Delta\vec{p} = \Delta t q(\vec{E} + \vec{v} \times \vec{B})$$

Use time-centered or “leapfrog” scheme:

- E and B evaluated at integer timesteps ( $E^n$  and  $B^n$ )
- p is evaluated at half-integer time steps ( $p^{n-1/2}$  and  $p^{n+1/2}$ ) (Accuracy goes as  $(\Delta t)^2$  rather than  $(\Delta t)$ .)



How should we apply the “push” from the E and B fields?

- Apply  $1/2$  of the E push
- Apply B (which acts as a pure rotation of the momentum vector)
- Apply remaining  $1/2$  of E push

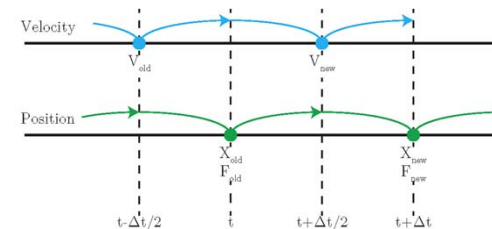
$$\vec{p}^- = \vec{p}^{n-1/2} + \frac{1}{2} \Delta t q \vec{E}^n$$

$$\vec{p}^+ = \vec{p}^- + \Delta t q \frac{\vec{p}^+ + \vec{p}^-}{2} \times \vec{B}^n$$

$$\vec{p}^{n+1/2} = \vec{p}^+ + \frac{1}{2} \Delta t q \vec{E}^n$$

$$\vec{x}^{n+1} = \vec{x}^n + \frac{\vec{p}^{n+1/2}}{\gamma^{n+1/2}} \Delta t$$

The cross-product is cast in a form that is efficient to evaluate and may involve approximations such as Taylor series expansion of required trig functions.

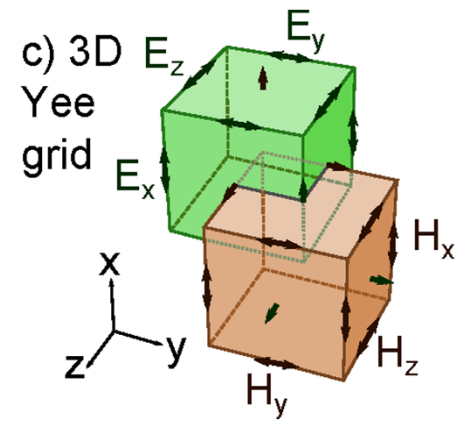
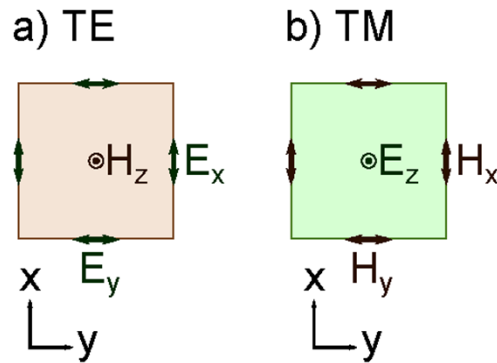


J. Boris, “Relativistic plasma simulation-optimization of a hybrid code”, Proceedings of the 4th Conference on Numerical Simulation of Plasmas. Naval Res. Lab., Washington, D.C., pages 3–67, 1970.

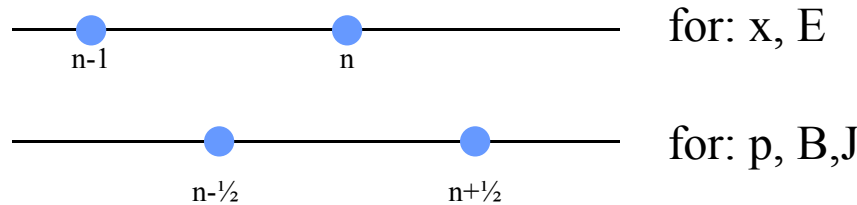
# Field Advance

$$\frac{\partial \vec{B}}{\partial t} = -\vec{\nabla} \times \vec{E}$$

$$\frac{\partial \vec{E}}{\partial t} = \frac{1}{\mu_0 \epsilon_0} \vec{\nabla} \times \vec{B} - \frac{1}{\epsilon_0} \vec{J}$$



Now we require spatial derivatives of the fields so, analogous to the leap frog approach, it is common to define E & J and B using different but interleaved spatial grids. For the time derivatives:



$$\frac{B_x|_{i,j+\frac{1}{2},k+\frac{1}{2}}^{n+1} - B_x|_{i,j+\frac{1}{2},k+\frac{1}{2}}^n}{\Delta t} = \frac{E_y|_{i,j+\frac{1}{2},k+1}^{n+\frac{1}{2}} - E_y|_{i,j+\frac{1}{2},k}^{n+\frac{1}{2}}}{\Delta z} - \frac{E_z|_{i,j+1,k+\frac{1}{2}}^{n+\frac{1}{2}} - E_z|_{i,j,k+\frac{1}{2}}^{n+\frac{1}{2}}}{\Delta y}$$

and similarly for the other components and for E.

$$\vec{\nabla} \cdot \vec{E} = \frac{\rho}{\epsilon_0}$$

We require these be satisfied as initial conditions, perhaps using a static field solver initially if necessary.

$$\vec{\nabla} \cdot \vec{B} = 0$$

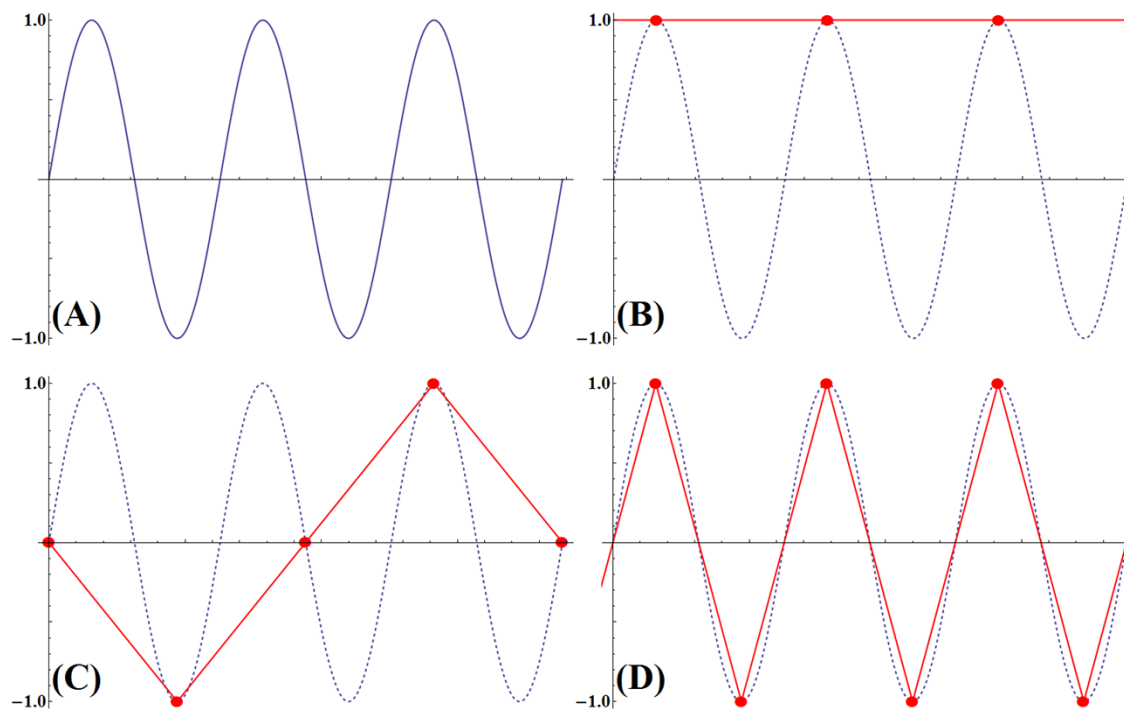
# Outline



1. Goals, Scope and Motivation
2. **Particle-in-cell Method**
  - a) Fundamentals – the basic method
  - b) Constraints**
  - c) Other aspects of a working simulation
  - d) Issues for the Laser Plasma Interaction
3. Case Studies

# Constraints on time step, cell size, particle count

- *Stability*. Small errors will occur because we are using difference equations, inevitability of numerical error and often other approximations. Will these errors grow?
- *Accuracy*. How well are the equations of motion solved? A simple error comes from undersampling an important physical process.



A sine wave of frequency  $f$  and the result of sampling it at  $f$ ,  $4f/3$ ,  $2f$ .

# Effect of the grid

We've noted the loss of translational invariance, already.


There are effects analogous to those of a crystal lattice and an analysis in k-space is indicated.

$$\rho(k) \equiv \Delta x \sum_j \rho_j e^{-kx} \quad \text{for the grid node charge density in 1D.}$$

The  $\rho_j$  are determined by the macroparticle positions, weights and shape function  $S(x-x_j)$ .

$$\rho(k) = q \sum_p S(k_p) n(k_p) \quad \text{where } n(x) \text{ is the particle number density and } k_p = k - k_g.$$

$k_g = 2\pi/\Delta x$  is the grid wavenumber.



The diagram shows a horizontal line representing a 1D grid. There are four vertical tick marks on the line, representing grid nodes. Three red circles representing particles are placed on the line. The first red circle is positioned between the first and second tick marks. The other two red circles are positioned between the second and third tick marks, with a small gap between them.

The grid density at  $k$  is coupled to  $n(k)$ , but also to other  $k_p$  depending on the width of  $S(k_p)$ . A shape function with a large enough extent in  $x$  will have a narrow distribution in  $k$ -space, effectively truncating the sum to the first Brillouin Zone and yielding:  $\rho(k) = q n(k)$

This modifies the vacuum plasma dielectric constant and dispersion relations from their usual expressions:

$$\epsilon = 1 - \frac{\omega_p^2}{\omega^2}$$

$$\omega^2 = k^2 c^2 + \omega_p^2$$



# Courant Condition

If we try to represent an EM planewave on the grid:

$$\vec{E}(\vec{x}, t) = \vec{E}_o \exp[i(\vec{k} \cdot \vec{x} - \omega t)]$$

$$\vec{B}(\vec{x}, t) = \vec{B}_o \exp[i(\vec{k} \cdot \vec{x} - \omega t)]$$

The usual relations from the Maxwell curl equations become modified on the grid:

$$\begin{array}{ccc} \omega \vec{B} = \vec{k} \times \vec{E} & \longrightarrow & \Omega \vec{B} = \vec{k} \times \vec{E} \\ \omega \vec{E} = -\vec{k} \times \vec{B} & & \Omega \vec{E} = -\vec{k} \times \vec{B} \end{array}$$

Where:

$$\Omega = \omega \frac{\sin \omega \Delta t / 2}{\omega \Delta t / 2} \quad \kappa_x = k_x \frac{\sin k_x \Delta x / 2}{k_x \Delta x / 2} \quad \text{etc.} \quad \begin{array}{l} \Delta t \text{ is the time step} \\ \Delta x, \text{ etc. are the cell sizes} \end{array}$$

Eliminating E and B:  $\Omega^2 = c^2 \kappa^2$  (instead of  $\omega^2 = c^2 k^2$ )

$$\left( \frac{\sin \frac{\omega \Delta t}{2}}{c \Delta t} \right)^2 = \left( \frac{\sin \frac{k_x \Delta x}{2}}{\Delta x} \right)^2 + \left( \frac{\sin \frac{k_y \Delta y}{2}}{\Delta y} \right)^2 + \left( \frac{\sin \frac{k_z \Delta z}{2}}{\Delta z} \right)^2$$

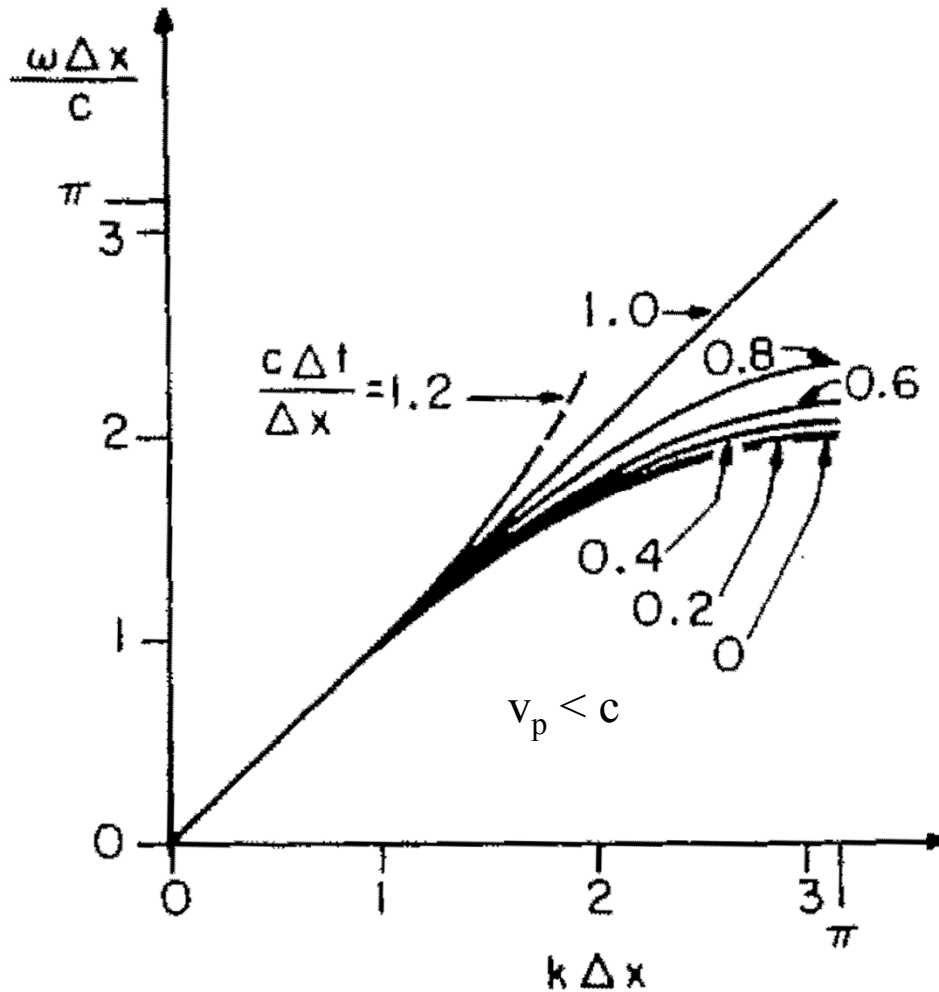
For real  $\omega$ , we require:

$$\left( \frac{1}{c \Delta t} \right)^2 > \left( \frac{1}{\Delta x} \right)^2 + \left( \frac{1}{\Delta y} \right)^2 + \left( \frac{1}{\Delta z} \right)^2$$

This imposes a maximum time step such that the light must not cross a cell in one step.

# Courant Condition

Vacuum dispersion solution of Maxwell's equations for propagation along x.



Relativistic particle can produce Cerenkov emission here

$$\left( \frac{\sin \frac{\omega \Delta t}{2}}{c \Delta t} \right)^2 = \left( \frac{\sin \frac{k_x \Delta x}{2}}{\Delta x} \right)^2$$

# More constraints on the time step

Possible relevant frequency (time) scales include

- laser carrier (and harmonics might be present)

Must resolve  $\lambda$

Courant condition applies:  $\Delta t < \Delta x/c$

But, also, grid dispersion

- plasma frequency

Not resolving this is inaccurate but, worse, there can also be stability issues.

- Cyclotron frequency

Similar

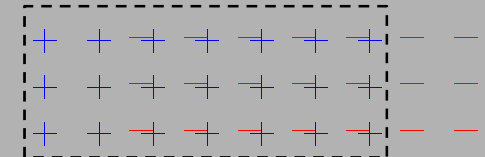
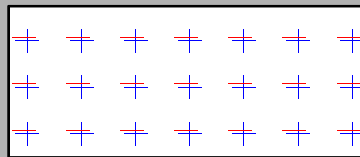
Langdon (and others) found a stability requirement that applies to explicit finite difference schemes in the particle pusher. The instability is related to temporal aliasing analogous to the spatial effect we just looked at:

$$\exp(-i\omega_q t_n) = \exp\left(-i\omega t_n + iq \frac{2\pi}{\Delta t} t_n\right) = \exp(-i\omega t_n) \quad \text{for aliases } \omega_q \text{ of } \omega; n, q \text{ integers.}$$

For small perturbations in a cold plasma:  $\omega_p \Delta t \leq 2$

or  $\omega$  in the dispersion relation becomes imaginary:  $\omega = \vec{k} \cdot \vec{v} \pm \frac{2}{\Delta t} \sin^{-1} \frac{\omega_p \Delta t}{2}$

Recall:  $\omega_p = \sqrt{ne^2 / \epsilon_0 m}$



# Heating instability

Recall:

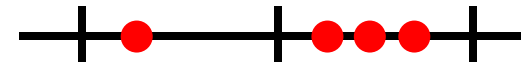
$$\rho(k) = q \sum_p S(k_p) n(k_p) \quad \text{where } n(x) \text{ is the particle number density and } k_p = k - k_g.$$

$k_g = 2\pi/\Delta x$  is the grid wavenumber.

- $n(x)$  determined particle positions and can have large extent in  $k$ -space
- $\rho$  (or  $J$ ) is what interacts with the fields and  $\rho(k)$  will couple to  $E(k)$ .

$n(x) = \text{pure sinusoid} \Rightarrow \rho(k)$  still has many  $k_p$  (unless filtered by  $S$ )  $\Rightarrow$  feeds back to  $n(x)$

$n(x)$  perturbations with  $k\Delta x > \pi$  contribute to  $\rho$  for  $k\Delta x < \pi$  because  $k$ 's differing by  $k_g$  look the same on the grid.



- $S(x)$  that is large in extent will have narrow  $S(k_p)$

Recall from FT:  $g(x) = \frac{1}{\sigma\sqrt{2\pi}} \exp\left(-\frac{x^2}{2\sigma^2}\right) \Leftrightarrow G(k) = \exp\left(-\frac{k^2\sigma^2}{2}\right)$

The real part of the dielectric function need not be sensitive to the aliasing.

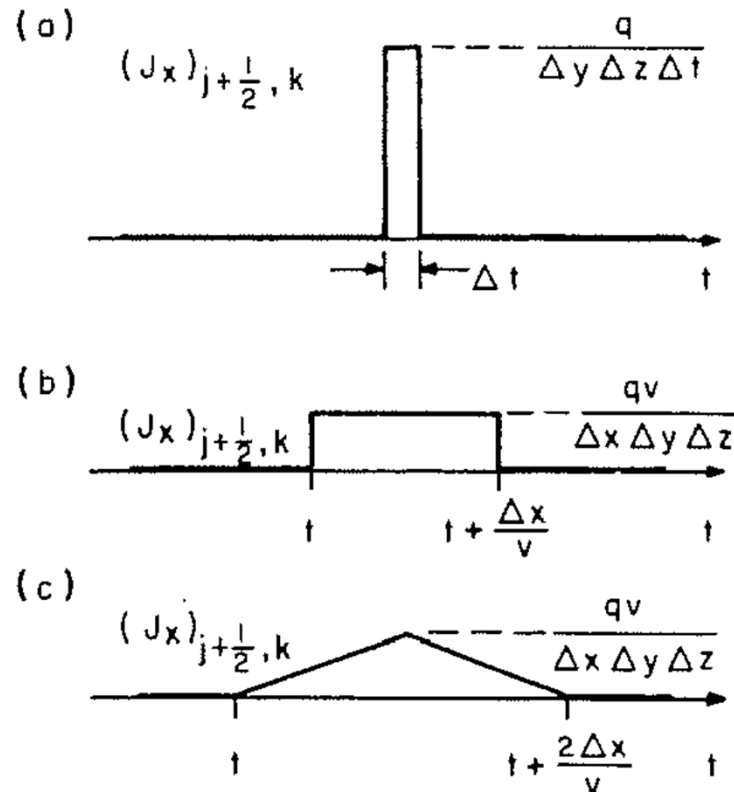
The imaginary part can actually change sign due to  $k_p$  with opposite sign of  $k$ .

Essentially, Landau damping becomes poor for components with large  $k_p$  yielding instability.

A rule of thumb is:  $\Delta x > 2-3 \lambda_D$  to avoid this for 1<sup>st</sup> order weighting

# Noise

We've seen that the weighting scheme (choice of S) effects noise.



Current impulse from a slow charge from three weighting approaches. Noise spectra fall off as  $\omega^0$ ,  $\omega^{-1}$ ,  $\omega^{-2}$ .

The number of macroparticles also does.

At solid density and 10 macroparticles/cell you'll have 10% of solid density changes each time a macroparticle crosses the middle of a cell for 0<sup>th</sup> order weighting.

It can also be shown for a plasma wave:

$$\left| \frac{e\Phi}{T_e} \right|_{th} = \frac{1}{\sqrt{N} k \lambda_D}$$

where N is the number of electron macroparticles contributing to the wave.

Phase space statistics are also an issue. Frequently, this is difficult to determine until after the simulation has run.

# Outline

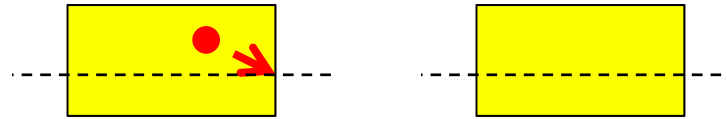
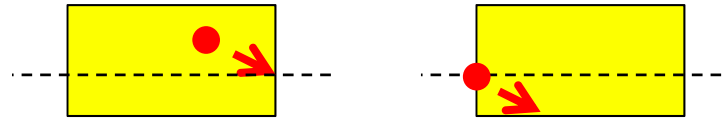


1. Goals, Scope and Motivation
2. **Particle-in-cell Method**
  - a) Fundamentals – the basic method
  - b) Constraints
  - c) **Other aspects of a working simulation**
  - d) Issues for the Laser Plasma Interaction
3. Case Studies

# Boundary Conditions and adding energy to the simulation

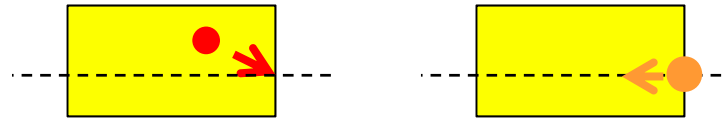
BC for fields:

- periodic
- absorbing
- conducting

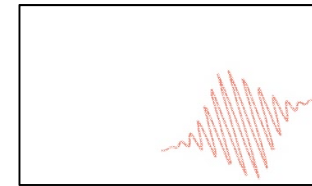
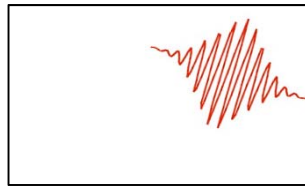


BC for particles:

- periodic
- absorbing
- thermal



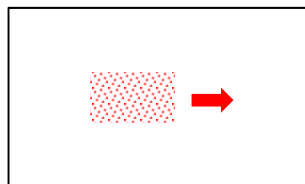
All boundary conditions impose restrictions on the simulation, and they may not work well. EM waves can partially reflect at an absorbing boundary, especially at grazing incidence.



Laser model:



Injection:





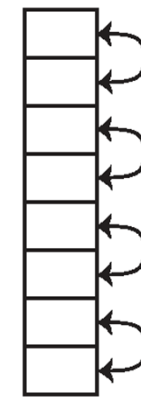
# Collision models

Two models for collisions are:

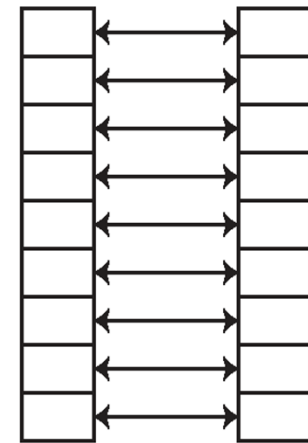
- Binary collision – sampling approach
- Jones algorithm – grid approach

## Binary

- cell particles grouped in pairs
- elastic collision in center-of-mass frame
- probability derived from the Spitzer collision rate
- scattering angle  $\theta$  and random azimuthal angle
- transform to lab frame



within species



between species

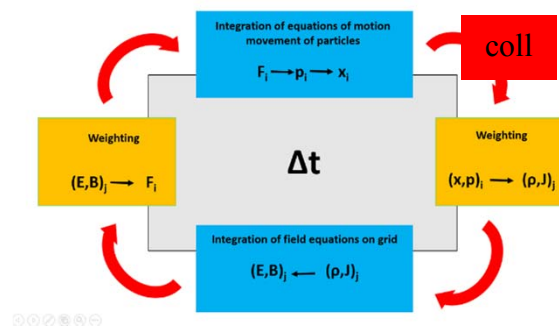
$$\sin\theta = \frac{2\delta}{1 + \delta^2}$$

$\delta$  is sampled from a Gaussian dist. with variance:

$$\langle \delta^2 \rangle = \frac{q_\alpha q_\beta n_L \Lambda}{8\pi \epsilon_0^2 m^2 u^3} \Delta t$$

## Jones

- find momentum and temperature per species per cell
- sample as Maxwell-Boltzmann distribution
- scatter each macroparticle



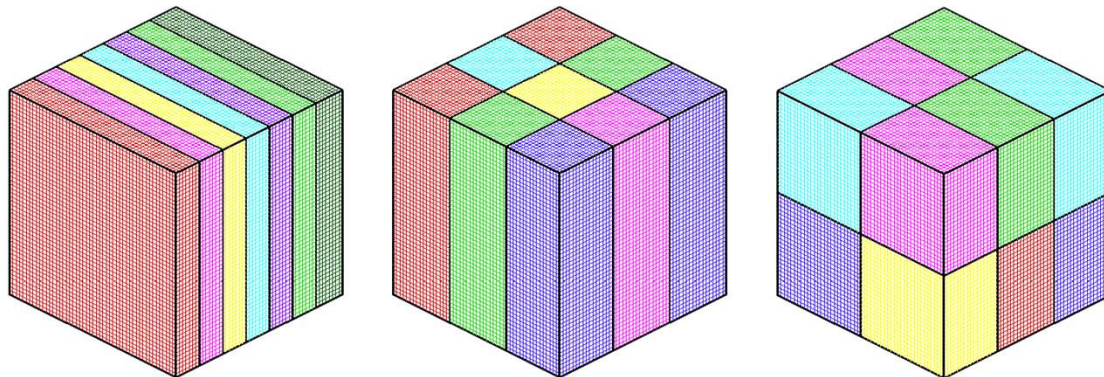
T. Takizuka and H. Abe, *Journal of Computational Physics* **25**, 205 (1977).

M. E. Jones, D. S. Lemons, R. J. Mason, V. A. Thomas, and D. Winske, *Journal of Computational Physics* **123**, 169 (1996)

# Multiprocessing (High Performance Computing)

Each processor is assigned part of the grid.

It “owns” the nodes and particles that happen to be in its domain.



The solution to the field equations requires knowing the fields of nearest neighbors.

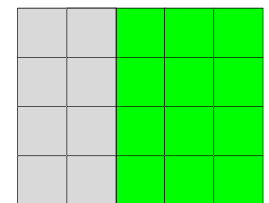
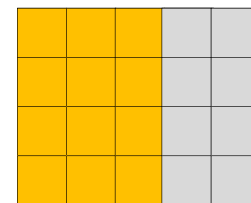
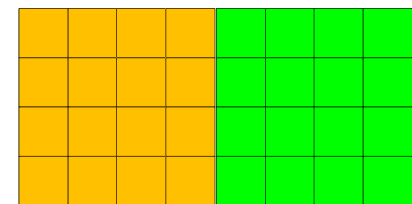
Similarly, interpolation to the particles. Note form of equations (using electrostatic eqns):

$$\nabla^2 \phi = -\frac{\rho}{\epsilon_0}$$

$$\frac{\phi_{j-1} - 2\phi_j + \phi_{j+1}}{(\Delta x)^2} = -\frac{\rho_j}{\epsilon_0}$$

$$\mathbb{A}\bar{\phi} = -\frac{(\nabla x)^2}{\epsilon_0} \bar{\rho}$$

$$\begin{pmatrix} a_1 & b_1 & & & & \\ c_1 & a_2 & b_2 & & & \\ & c_2 & \ddots & \ddots & & \\ & & \ddots & \ddots & b_{n-1} & \\ & & & c_{n-1} & a_n & \end{pmatrix}$$



Communication via some protocol, for example, MPI.

# Diagnostics



## Consider

A 2D  $100 \mu\text{m} \times 100 \mu\text{m}$  grid with 20 cells per  $\mu\text{m} = 4 \times 10^6$  cells

50 macroparticles/cell (of all species) in  $\frac{1}{2}$  the cells initially =  $1 \times 10^8$  particles

2 ps of simulation time with 0.13 fs time steps ( $T/20$  @ 800 nm) = 15,000 time steps

(these numbers are conservative, simulations much larger than this are routine)

## Space assuming single precision dump for 1 time step

Fields – 6 components =  $\sim 90$  MB

Particles – 5 element phase space = 2 GB

## Must restrict the output

- Only periodic or selected dump times
- Reduced spatial resolution, particle sampling/particle tagging
- Only the field components or phase space elements needed
- Use reduced measures
  - temperature, density, phase space map instead of particles
  - extraction plane or border
  - tracer particles

## Diagnostic outputs (perhaps once per time step or few time steps)

- measures of energy (total, particle, field, non-conservation)
- measures of behavior (maximum plasma frequency, collision rates)
- measure of processor performance (time spent on different tasks)

## There are important issues I haven't mentioned and many different kinds of PIC

- Current correction
- Damping and filtering
- Sub-cycling
- Sub-gridding
- Particle management

### Varieties of PIC

- Electrostatic PIC
- Electromagnetic PIC
- Gravitational PIC
- Implicit solvers
- Hybrid codes incorporating fluid models
- Other variations
  - Incorporation of Ohm's Law directly (not via collisions)
  - PIC combined with other solvers by region or dimension
  - Hydro codes that incorporate PIC

# Outline



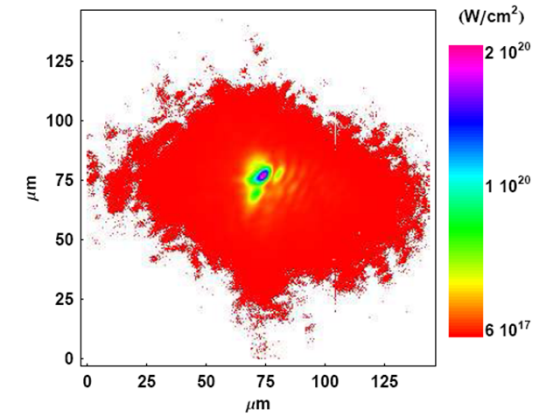
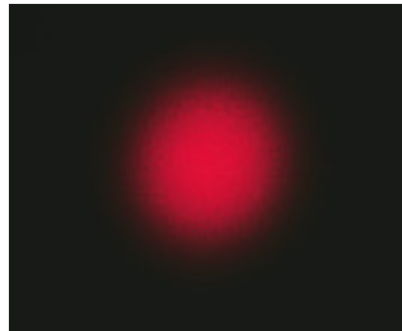
1. Goals, Scope and Motivation
2. **Particle-in-cell Method**
  - a) Fundamentals – the basic method
  - b) Constraints
  - c) Other aspects of a working simulation
  - d) Issues for the Laser Plasma Interaction**
3. Case Studies

# Modeling real experiments

Assume we want to model a laser and not use an injection. Assume a solid target.  
Some choice of dimensionality is made based on the problem and computing resources.

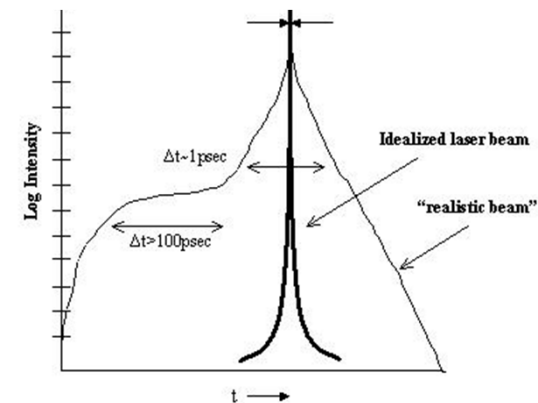
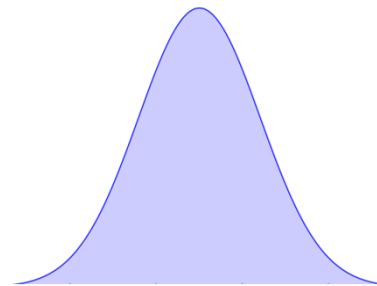
What spatial scales need to be resolved on physical grounds?

- wavelength
- Debye length
- skin depth ( $c/\omega_p$ )
- target thickness
- target surface structure



Temporal/frequency scales?

- pulse carrier (harmonics?)
- plasma frequency
- cyclotron frequency



Size of grid needed and duration of simulation?

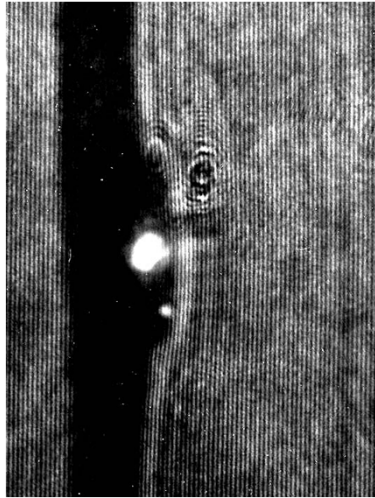
- size of target
- vacuum border or support structures
- pulse length
- particle travel times

Order of magnitude:

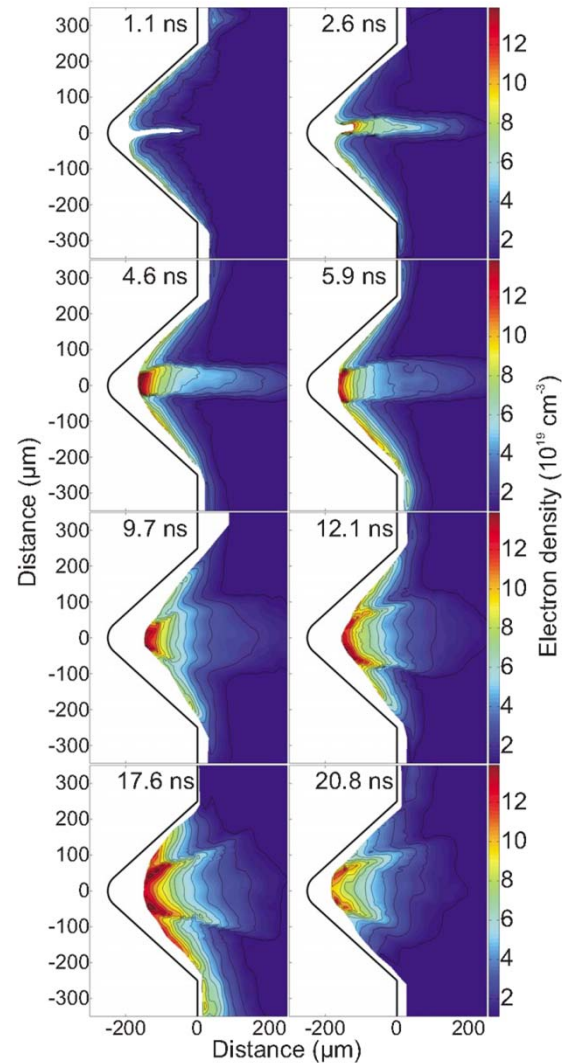
- $\lambda$ : 1  $\mu\text{m}$
- target dimensions: 10 nm to 1 mm  
(can go to cm; gas targets tend to be bigger)
- pulse, travel: fs to nm



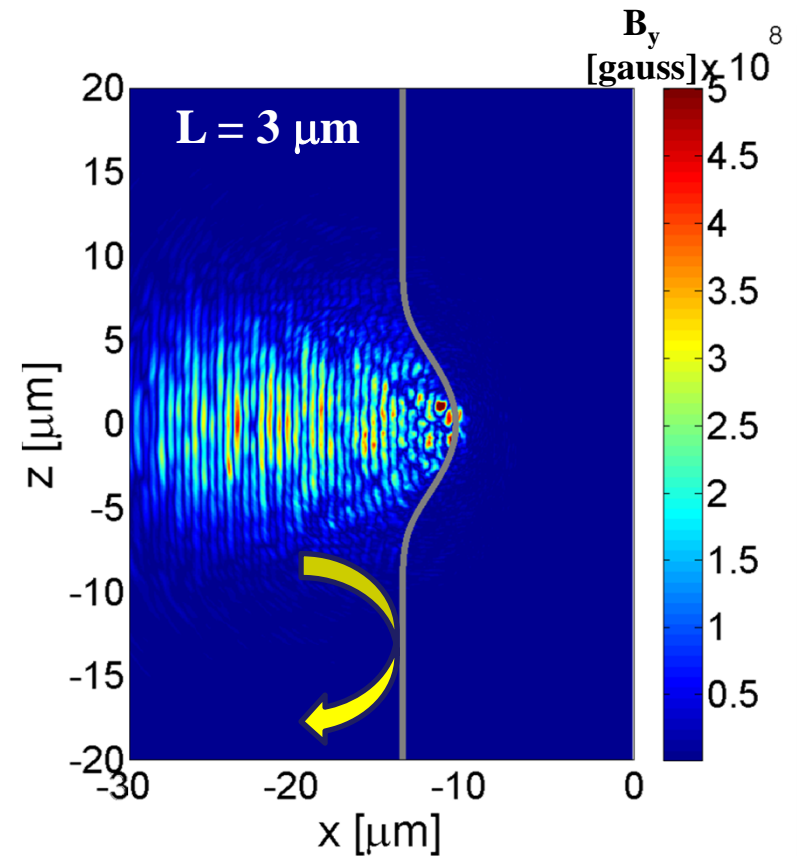
# Pre-pulse and pre-plasma and the LPI



Interferogram from Daniel Hey (thesis).



Irradiation by 0.8 J, 120 ps Ti:Sapphire laser with  $I = \sim 10^{12}$  W/cm<sup>2</sup>, derived from measured interferograms. Grava et al, PRE 78, 016403 (2008).



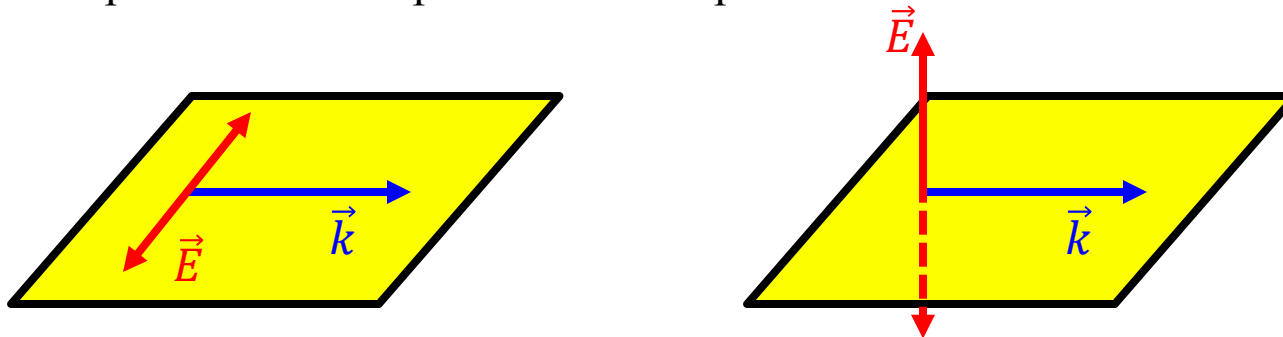
PIC simulations for 110 fs,  $10^{19}$  W/cm<sup>2</sup> Gaussian spatial profile pulse incident on singly charged ion. (Schumacher et al, POP 18, 013102 (2011)).

$$n_c = \frac{\epsilon_0 m}{e^2} \omega_L^2$$

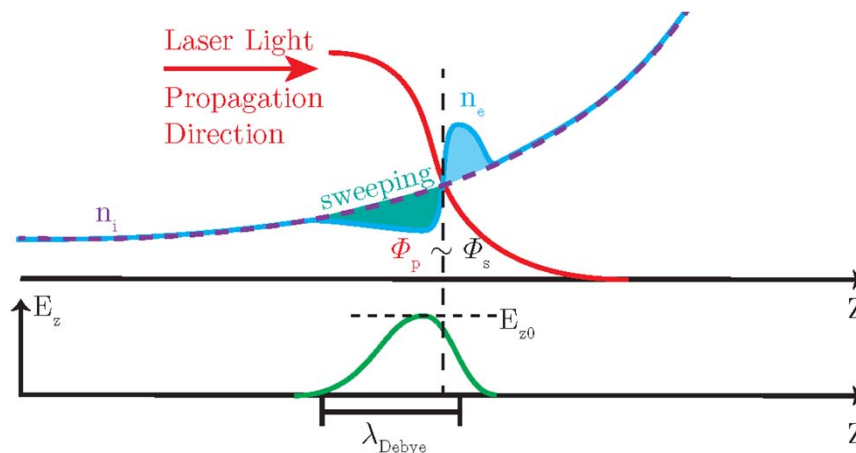
## 2D and 1D LPI

Polarization: linear, elliptical, circular can be supported in 1D, 2D, 3D but this is problematic for anything other than 3D.

2D3V and linear polarization: in-plane or out-of-plane?



Charges can accelerate in any direction, but they can't move in the virtual direction. This exaggerates or diminishes many effects.



Y. Sentoku, et al., "High energy proton acceleration in interaction of short laser pulse with dense plasma target", *Physics of Plasmas* **10**, 2009 (2003).



# Numerical choices

## Basic constraints:

- Debye length:  $\Delta x < 3 \lambda_D$
- Plasma frequency:  $\omega_p \Delta t < 2$
- Courant Condition:  $c \Delta t < \Delta x$   
(but also dispersion constraints)

$$\lambda_D = \sqrt{\epsilon_0 kT / ne^2}$$

$$\omega_p = \sqrt{ne^2 / \epsilon_0 m}$$

## But these can be mitigated:

- Debye length: run at high T or low n, use large particle shape, energy conserving algorithms
- Plasma frequency: run at low n
- implicit solvers can relax all of these constraints
- instabilities have growth times – perhaps your simulation will finish soon enough

## Speed-ups (usually with consequences):

- variable time step
- varying or variable grid
- variable macroparticle count
- restricted grid dimension, simulation duration or dimensionality
- more processors (no adverse consequences for the simulation, but costly and saturates)

## Convergence tests:

- time step
- spatial resolution
- particle count

# Outline



1. Goals, Scope and Motivation
2. Particle-in-cell Method
3. **Case Studies**
  - a) Petawatt laser pulses and overdense plasmas
  - b) Relativistic Kelvin-Helmholtz instability

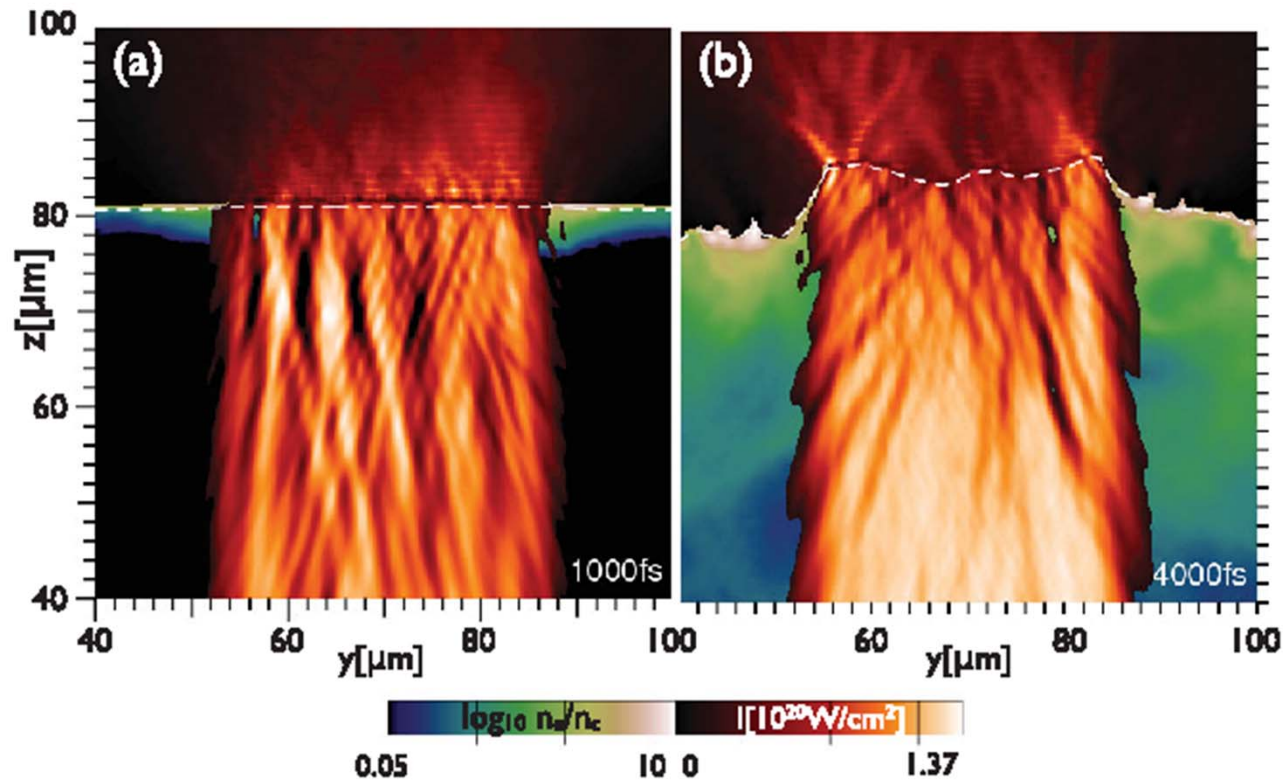


FIG. 1 (color). Relativistic petawatt laser pulse interacting with overdense plasma at 1 ps (a) and at 4 ps (b); the laser pulse is injected at  $z = 0$ , and plasma is initially at  $z > 80 \mu\text{m}$ . Energy flux density along  $z$  (in red) shows continuously high conversion from the laser into a relativistic electron beam. The dashed line at  $n_e = 10n_c$  shows deformation and motion of the absorption layer. Expansion of underdense plasma into vacuum (in green) is evident.

# Petawatt laser pulses and overdense plasmas

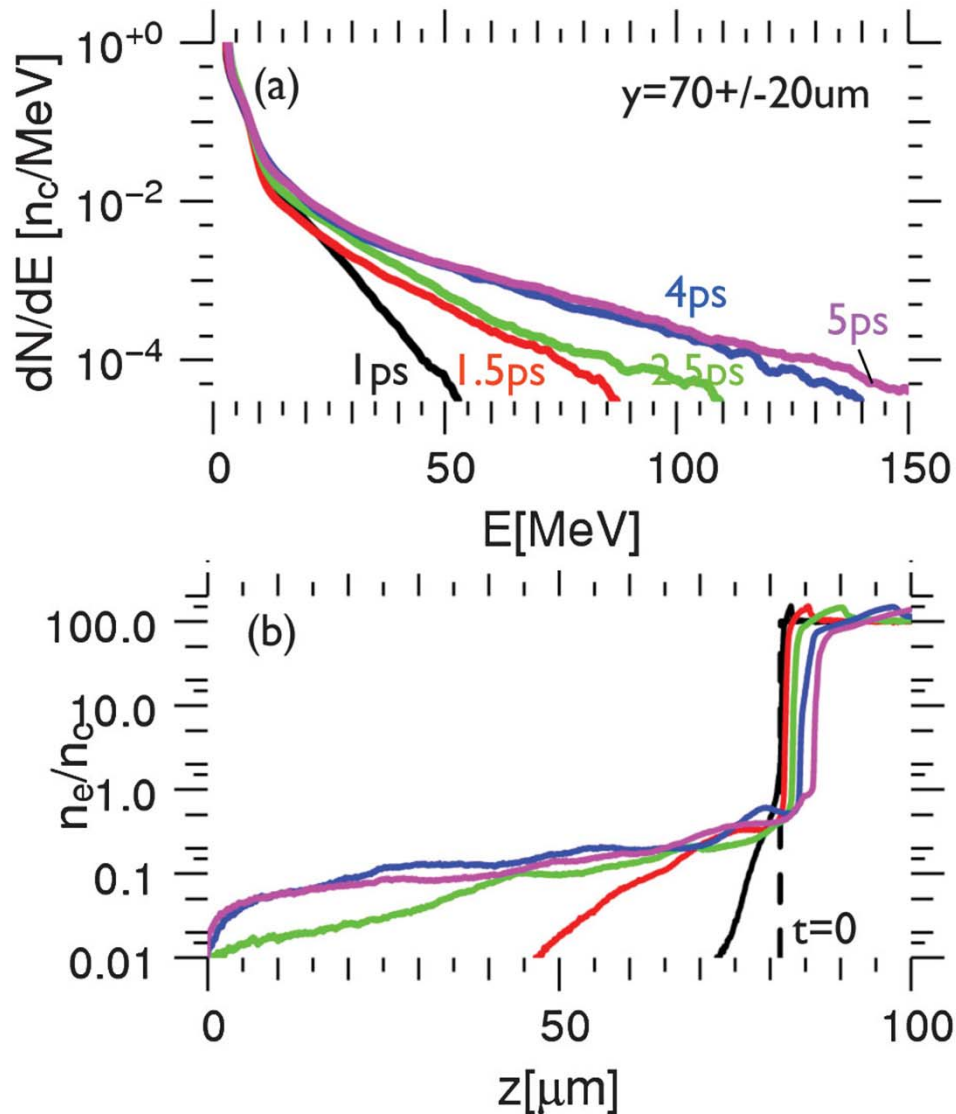


FIG. 3 (color). (a) Energy spectra of laser-generated electrons consist of three energy groups, with a high-energy tail that asymptotes at 4 ps; (b) similarly, electron density profiles, averaged across the laser spot, asymptote towards a near plateau at 4 ps; colors in (a) and (b) for the same time steps match.

The pre-plasma profile reshapes dramatically over  $\sim 3$  ps. The classical critical surface moves significantly.

This changes hot electron generation correspondingly, so there is no one “ $T_{\text{hot}}$ ”.

# Kelvin-Helmholtz Instability

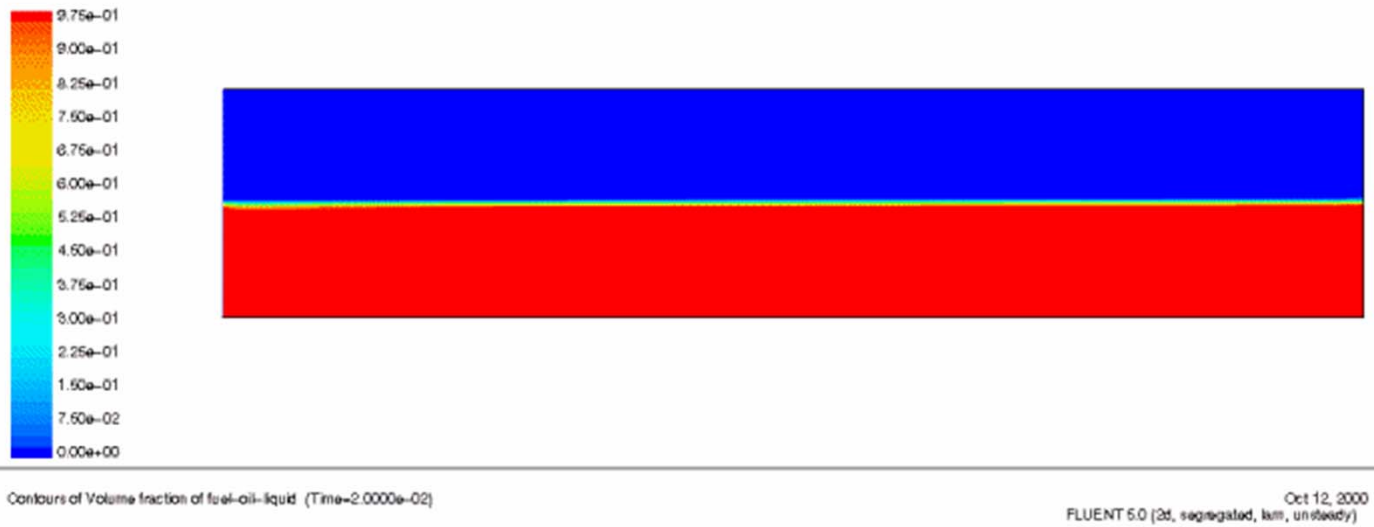
A fundamental instability in plasmas first observed in ordinary fluids. It requires a shear between two fluids (or within the same fluid).

In a plasma, shear forces give rise to filaments that amplify a magnetic field that enhances the perturbation. This can lead to a periodic density and field modulation along the interface.



[https://en.wikipedia.org/wiki/Kelvin-Helmholtz\\_instability](https://en.wikipedia.org/wiki/Kelvin-Helmholtz_instability)

This occurs in astrophysical environments when a relativistic jet passes through a background plasma. The emitted radiation by the plasma electrons is a primary diagnostic.



Animation of two immiscible fluids, with the faster stream on top, both flowing to the right.

<http://hmf.enseiht.fr/travaux/CD0001/travaux/optmfn/hi/01pa/hyb72/kh/anim2.htm>

# Simulations using PIConGPU

## Radiative Signatures of the Relativistic Kelvin-Helmholtz Instability

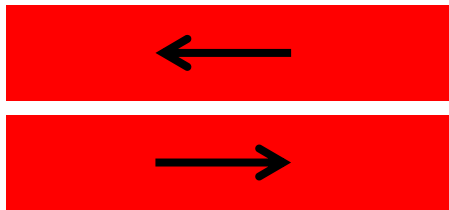
<p><b>M. Bussmann</b> Helmholtz-Zentrum Dresden – Rossendorf Bautzner Landstrasse 400 01328 Dresden, Germany +49 351 260-2616 m.bussmann@hzdr.de</p>	<p><b>H. Burau</b> Helmholtz-Zentrum Dresden – Rossendorf Bautzner Landstrasse 400 01328 Dresden, Germany +49 351 260-3377 h.burau@hzdr.de</p>	<p><b>T.E. Cowan</b> Helmholtz-Zentrum Dresden – Rossendorf Bautzner Landstrasse 400 01328 Dresden, Germany +49 351 260-2270 t.cowan@hzdr.de</p>	<p><b>A. Debus</b> Helmholtz-Zentrum Dresden – Rossendorf Bautzner Landstrasse 400 01328 Dresden, Germany +49 351 260-2619 a.debus@hzdr.de</p>
<p><b>A. Huebl</b> Helmholtz-Zentrum Dresden – Rossendorf Bautzner Landstrasse 400 01328 Dresden, Germany +49 351 260-3639 a.huebl@hzdr.de</p>	<p><b>G. Juckeland</b> Technische Universität Dresden Center for Information Services and High Performance Computing 01062 Dresden, Germany +49 351 463-39671 guido.juckeland@tu- dresden.de</p>	<p><b>T. Kluge</b> Helmholtz-Zentrum Dresden – Rossendorf Bautzner Landstrasse 400 01328 Dresden, Germany +49 351 260-2618 t.kluge@hzdr.de</p>	<p><b>W.E. Nagel</b> Technische Universität Dresden Center for Information Services and High Performance Computing 01062 Dresden, Germany +49 351 463-35450 wolfgang.nagel@tu- dresden.de</p>
<p><b>R. Pausch</b> Helmholtz-Zentrum Dresden – Rossendorf Bautzner Landstrasse 400 01328 Dresden, Germany +49 351 260-2616 r.pausch@hzdr.de</p>	<p><b>F. Schmitt</b> Technische Universität Dresden Center for Information Services and High Performance Computing 01062 Dresden, Germany +49 351 463-39671 felix.schmitt@tu- dresden.de</p>	<p><b>U. Schramm</b> Helmholtz-Zentrum Dresden – Rossendorf Bautzner Landstrasse 400 01328 Dresden, Germany +49 351 260-2618 u.schramm@hzdr.de</p>	<p><b>J. Schuchart</b> Oak Ridge National Lab PO Box 2008 MS-6164 Oak Ridge, TN 37831-6164 +1 865 241-6293 schucharj@ornl.gov</p>
<p><b>R. Widera</b> Helmholtz-Zentrum Dresden – Rossendorf Bautzner Landstrasse 400 01328 Dresden, Germany +49 351 260-3543 r.widera@hzdr.de</p>			

3D Grid: 480 x 46 x 46 skin depths  
 Simulation volume: 8000 x 768 x 768 cells  
 Particles: 8 protons and 8 electrons / cell (75 billion particles)  
 Time steps: 2000 ( $62 \lambda_p$  in duration)  
 Resolution: 0.06 skin depths ( $\omega_p/c$ )

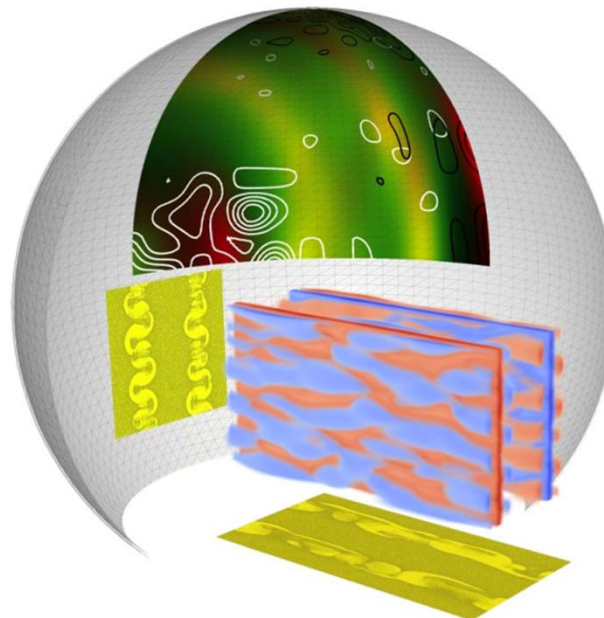
Radiation calculated (energy per unit solid angle and frequency) using LW potentials.

Yee solver, Boris pusher, TSC shape function (2<sup>nd</sup> order with continuous value and 1<sup>st</sup> derivative. See Hockney and Eastwood, p 311), periodic boundary conditions in all dimensions.

>7 PFLOPs (double precision)  
 running on 18,000 nodes.  
 About 17-19 s per time step.



(in rest frame of streams)



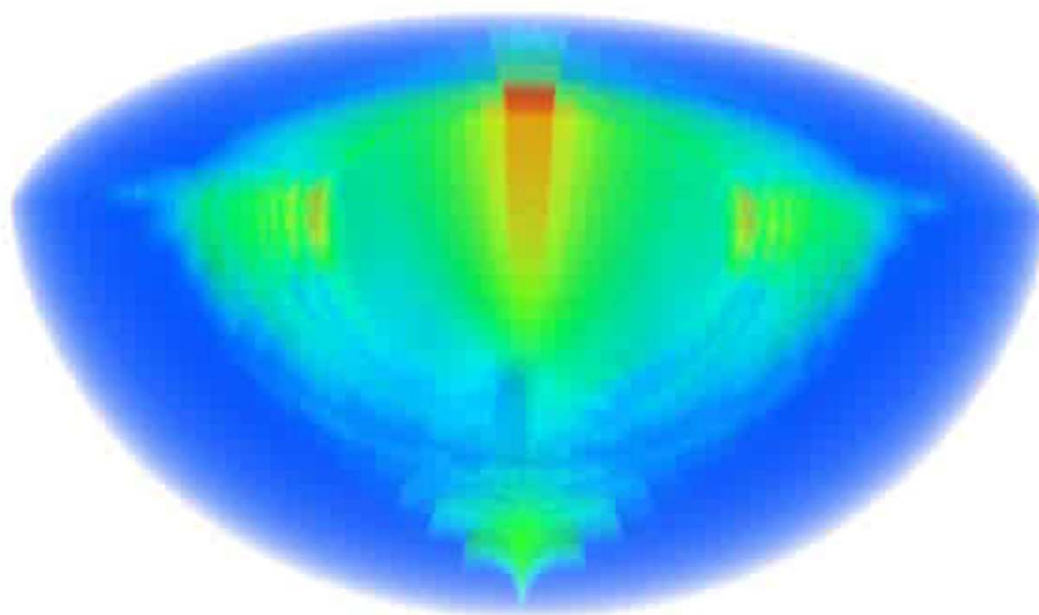
Magnetic fields (blue,red)  
 Electron density projection (yellow)  
 Radiation emitted (projection on sphere)



## Radiative Zones of the Relativistic Kelvin-Helmholtz Instability

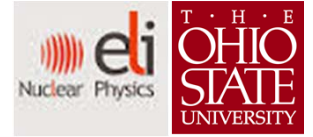
Colors distinguish electron acceleration, or the change in an electron's speed and direction, occurring in passing plasma streams. Red indicates large electron acceleration leading to strong radiation emission. Visualization by Dave Pugmire, ORNL.  
<https://www.olcf.ornl.gov/2013/11/11/simulations-of-plasma-turbulence-model-the-inner-workings-of-cosmic-phenomenon/>

# Radiation





# Acknowledgements



OSU students, former students and colleagues Sheng Jiang, Frank King, Andy Krygier and Rick Freeman.

Michael Bussmann (HZDR) and his PIconGPU development team.

ELI-NP